Kaon meson condensate in neutron star matter including hyperons

Fu Ma,[1] Wenjun Guo,[1] and Chen Wu[2,*]

[1]*College of Science, University of Shanghai for Science and Technology, Shanghai 200093, China*

[2]*Shanghai Advanced Research Institute, Chinese Academy of Sciences, Shanghai 201210, China*

(Received 29 August 2021; revised 20 November 2021; accepted 18 January 2022; published 31 January 2022)

The recent measurement of the mass of neutron stars (PSR J1614−2230, PSR J0348+0432, MSP J0740+6620) restricts the lower limit $\sim 2M_\odot$ of the maximum mass of such compact stars, making it possible for dense matter to exist in massive stars. The relativistic mean-field theory with parameter sets FSUGold including kaon condensation is used to describe the properties of neutron stars in β equilibrium. Through careful choice of the parameter of the σ-cut c_σ, we are able to produce a maximum mass neutron star with kaon condensation heavier than $2M_\odot$, and we find that the parameter Λ_v of the $\rho-\omega$ interaction term in this model has a significant effect on K^- condensation. In the case of using the σ-cut scheme, K^- condensation occurs only when the $\rho-\omega$ interaction Λ_v is switched off.

DOI: 10.1103/PhysRevC.105.015807

I. INTRODUCTION

Born as a result of supernova explosions, neutron stars are highly condensed stellar remnants. A typical neutron star has a mass of the order of the solar mass, but its radius is only around $10 \sim 12$ km. The internal matter composition and equation of state (EOS) of compact stars are restricted by recent gravitational wave observations. The massive NSs observed, e.g., PSR J1614−2230 with $M = 1.908 \pm 0.016 M_\odot$ [1–4], have established strong constraints on the EOS of nuclear matter. PSR J0348+0432 with $M = 2.01 \pm 0.04 M_\odot$ [5], MSP J0740+6620 with $M = 2.08^{+0.07}_{-0.07} M_\odot$ [6,7], and radius $12.39^{+1.30}_{-0.98}$ km obtained from NICER data [8], have strengthened the already stiff constraints on the EOS. The observation of gravitational waves is another crucial source of information about NS matter; the recent GW190814 event observed by the LIGO–Virgo Collaboration (LVC) from a coalescence of a black hole and a lighter companion sets the mass of the former to be $23.2^{+1.1}_{-1.0}\ M_\odot$ and that of the latter to be $2.59^{+0.08}_{-0.09}\ M_\odot$ [9]. It is unclear whether the lighter companion star is a neutron star or a black hole. So far, the study of neutron stars has been used as one of the important methods for studying strong interactions in dense nuclear matter, and it is still a research hot spot of nuclear celestial bodies [10,11]. It has gradually been discovered that only considering basic nucleon, neutrons, and protons is not enough in the study of neutron stars. In fact, the inner cores of the neutron stars are sources of speculation, some of the possibilities being the appearance of hyperons [12,13], only quarks [14–18], or kaon condensates [19–22].

Kaplan and Nelson have suggested that the ground state of hadronic matter might form a negatively charged kaon Bose-Einstein condensation above a certain critical density [23,24]. In the interior of a neutron star, as the density of neutrons increases, the electronic chemical potential will increase to keep the matter in β equilibrium. When the electronic chemical potential exceeds the mass of muons, muons appear. And when the vacuum mass of the meson (pion, kaon) is exceeded, as the density increases, negatively charged mesons begin to appear, which helps to maintain electrical neutrality. However, the s-wave πN scattering potential repels the ground-state mass of the π meson and prevents the generation of the π meson [25]. The effective mass of the K^- meson is decreased because of the interaction with the nucleon. If the K^- meson energy intersects with the electron chemical potential at a certain density, then K^- will be more advantageous than electrons as a neutralizer for positive charges. The very interaction that reduces the kaon energy modifies the nucleons with which they interact, and this will open the possibility of the appearance of kaon condensates.

Although many scholars have proposed various phenomenological models based on density functional theory and realistic nuclear potential to explain, the interaction of particles at such high densities is not known precisely. To get the EOS of the neutron star matter, the RMF theory is usually applied [26], which describes the interaction between baryons via the exchange of mesons [24,27,28]. The model determines the coupling parameters through the saturation properties of the nuclear matter and extends it to high density. It has achieved great success in the study of the nuclei and nuclear matter. There are many theoretical models within the RMF framework. In this paper, we are going to adopt the FSUGold model as an example [29]. The RMF theory with the parameter set FSUGold was proposed by Todd-Rutel and Piekarewicz [30–33]. It has achieved great success in study of the nuclear matter and the ground-state properties of some spherical nuclei [32]. However, when it is applied to study the EOS including hyperons, the maximum mass of the neutron stars obtained by this model is too small; the problem is that the EOS generated by the FSUGold model [13] is too soft.

*wuchenoffd@gmail.com

To describe nuclear matter at high density with the FSUGold model, some researchers have proposed a σ-cut scheme [34]. This scheme points out that if the mean-field self-interaction potential rises sharply in a narrow vicinity $n_0 \sim n$ of the value of mean fields corresponding to nuclear densities n_* [34], the nucleon effective mass saturates and the EOS stiffens, where n_0 is the nuclear saturation density. This procedure offers a simple way to stiffen the EOS at high densities without altering it at densities $n \leqslant n_0$. However, the effect of hyperons on neutron star matter is not included in study [34]. It is well known that the introduction of hyperon degrees of freedom leads to a softer EOS, thus producing a neutron star with a small mass. It leaves the open question of whether the σ-cut scheme is still effective when hyperons are considered. In addition, some scholars pointed out that exotic EOS cannot be ruled out by the observation of a $2M_\odot$ compact star [35]. In this article, we use the FSUGold model to study NS matter including hyperons and kaon condensates with the σ-cut scheme.

This paper is organized as follows. First, the theoretical framework is presented. Then we will study the effects of the σ-cut scheme. The kaon condensation will be considered, too. Finally, some conclusions are provided.

II. THEORETICAL FRAMEWORK

In this section, we introduce the FSUGold model to study the properties of the phase transition from hadronic to kaon condensed matter. For the baryons matter we have considered nucleons (n and p), and hyperons (Λ, Σ, and Ξ). The exchanged mesons include the isoscalar scalar meson (σ), the isoscalar vector meson (ω), and the isovector vector meson (ρ); the starting point of the extended FSUGold model is the Lagrangian density:

$$\begin{aligned}\mathcal{L} = &\sum_B \bar{\psi}_B[i\gamma^\mu\partial\mu - m_B + g_{\sigma B}\sigma - g_{\omega B}\gamma^\mu\omega_\mu - \frac{g_{\rho B}}{2}\gamma^\mu\vec{\tau}\cdot\vec{\rho^\mu}]\psi_B + \frac{1}{2}\partial_\mu\sigma\,\partial^\mu\sigma \\ &- \frac{1}{2}m_\sigma^2\sigma^2 - \frac{\kappa}{3!}(g_{\sigma N}\sigma)^3 - \frac{\lambda}{4!}(g_{\sigma N}\sigma)^4 - \frac{1}{4}F_{\mu\nu}F^{\mu\nu} + \frac{1}{2}m_\omega^2\omega_\mu\omega^\mu + \frac{\xi}{4!}\left(g_{\omega N}^2\omega_\mu\omega^\mu\right)^2 \\ &+ \frac{1}{2}m_\rho^2\vec{\rho}_\mu\cdot\vec{\rho}^\mu - \frac{1}{4}\vec{G}_{\mu\nu}\vec{G}^{\mu\nu} + \Lambda_v\left(g_{\rho N}^2\vec{\rho}_\mu\cdot\vec{\rho}^\mu\right)\left(g_{\omega N}^2\omega_\mu\omega^\mu\right) + \sum_l \bar{\psi}_l[i\gamma^\mu\partial\mu - m_l]\psi_l,\end{aligned} \tag{1}$$

where Λ_v is introduced to modify the density dependence of symmetry energy. All the eight lightest baryons (p,n, Λ^0, Σ^+, Σ^0, Σ^-, Ξ^0, Ξ^-) are included, as the two leptons, electron and muon. The terms m_σ, m_ω, and m_ρ are the masses of σ, ω, and ρ mesons, respectively. The antisymmetric tensors of vector mesons take the forms $F_{\mu\nu} = \partial_\mu\omega_\nu - \partial_\nu\omega_\mu$, $G_{\mu\nu} = \partial_\mu\rho_\nu - \partial_\nu\rho_\mu$. The isoscalar meson self-interactions (via κ, λ, and ξ terms) are necessary for the appropriate EOS of symmetric nuclear matter. $g_{\sigma N}$, $g_{\omega N}$, and $g_{\rho N}$ are the coupling constants between baryon and σ meson, baryon and ω meson, and baryon and ρ meson, respectively. In this paper, the operators of meson fields are replaced by their expectation values by the mean-field approximation.

With the increase of the density, the kaon condensation does appear in the interior of the neutron stars. We take the Lagrangian of kaon condensation as the same that is in Refs. [36,37], which reads

$$\mathcal{L}_K = D_\mu^* K^* D^\mu K - m_K^{*2} K^* K, \tag{2}$$

where $D_\mu = \partial_\mu + ig_{\omega K}\omega_\mu + i\frac{g_{\rho K}}{2}\tau_K\cdot\rho_\mu$ is the covariant derivative and the kaon effective mass is defined as $m_K^* = m_K - g_{\sigma K}\sigma$. The coupling constants between the vector meson and the kaon $g_{\omega K}$, $g_{\rho K}$ are determined by the meson SU(3) symmetry as $g_{\omega K} = g_{\omega N}/3$, $g_{\rho K} = g_{\rho N}$ [35]. The scalar coupling constant $g_{\sigma K}$ is fixed to the optical potential of the K^- at saturated nuclear matter:

$$U_K(\rho_0) = -g_{\sigma K}\sigma(\rho_0) - g_{\omega K}\omega(\rho_0), \tag{3}$$

which characterizes the kaon-nucleon interaction. Experiment studies show that the kaons experience a repulsive interaction in nuclear matter whereas antikaons experience an attractive potential [38,39]. Waas and Weise found an attractive potential for the K^- at the saturation nuclear density of about $U_K(\rho_0) = -120$ MeV [40]. Coupled channel calculations at finite density have yielded a value of $U_K(\rho_0) = -100$ MeV [41]. More recent self-consistent calculations with a chiral Lagrangian [42,43] and coupled channel calculation including a modified self-energy of the kaon [44] indicate that the kaon may experience an attractive potential with its depth about -80 MeV to even -50 MeV at the saturation density. Another calculation from the hybrid model [45] suggests the value of K^- optical potential to be in the range 180 ± 20 MeV at saturation density. In this paper, we carry out our calculations with a series of optical potentials ranging from -160 MeV to -120 MeV.

For the meson-hyperon couplings, we take those in the SU(6) quark model for the vector couplings constants:

$$g_{\rho\Lambda} = 0, g_{\rho\Sigma} = 2g_{\rho\Xi} = 2g_{\rho N}, \tag{4}$$

$$g_{\omega\Lambda} = g_{\omega\Sigma} = 2g_{\omega\Xi} = \frac{2}{3}g\omega N. \tag{5}$$

The scalar couplings are usually fixed by fitting hyperon potentials with $U_Y^{(N)} = g_{\omega Y}\omega_0 - g_{\sigma Y}\sigma_0$, where σ_0 and ω_0 are the values of the scalar and vector meson strengths at saturation density [46]. The Λ-N interaction was well studied and $U_\Lambda^N = -30$ MeV was obtained with bound Λ hypernuclear states [47,48]. One of the unsettled issues in hypernuclear physics is the Σ-N interaction in nuclear matter. An attractive potential was generally used in the past for Σ to be bounded in nuclear

TABLE I. $g_{\sigma K}$ determined for several U_K values in the FSUGold model.

U_K (MeV)	−120	−140	−160
$g_{\sigma K}$	0.6030	1.1775	1.7521

matter. However, a detailed scan for Σ hypernuclear states turned out to give negative results. The study of Σ^- atoms also showed strong evidence for a sizable repulsive potential in the nuclear core at $\rho = \rho_0$. Therefore, for the Σ-*N* interaction, we consider $U_\Sigma^{(N)} = -30$ MeV, as used in Ref. [48]. In addition, the Ξ-*N* interaction in nuclear matter is attractive with the potential $U_\Xi^{(N)} = -18$ MeV [35]. We take then such a value in our calculation. The $g_{\sigma K}$ can be related to the potential of kaon at the saturated density through Eq. (3). $g_{\sigma K}$ values corresponding to several values of U_K are listed in Table I.

By solving the Euler-Lagrangian equation of kaon we obtain equation of motion: $[D_\mu D^\mu + m_K^{*2}]K = 0$. We can then derive the dispersion relation for the Bose condensation of K^-, which reads

$$\omega_K = m_K - g_{\sigma K}\sigma - g_{\omega K}\omega - \frac{g_{\rho K}}{2}\rho. \tag{6}$$

With the increase of density, the energy ω_K of a test kaon in the pure normal phase can be computed as a function of the nucleon density. The kaon energy will decrease while the potential of kaon ($\omega_K = \mu_e$) increases with the density. When the condition $\omega_K = \mu_e$ is achieved, the kaon will occupy a small fraction of the total volume. The new meson field equations are then different from the normal phase because of the additional source terms and can be written explicitly as

$$\begin{aligned} m_\sigma^2\sigma + \frac{1}{2}\kappa g_{\sigma N}^3\sigma^2 + \frac{1}{6}\lambda g_{\sigma N}^4\sigma^3 &= \sum_B g_{\sigma B}\rho_B^S + g_{\sigma K}\rho_K, \\ m_\omega^2\omega + \frac{\xi}{6}g_{\omega N}^4\omega^3 + 2\Lambda_v g_{\rho N}^2 g_{\omega N}^2\rho^2\omega &= \sum_B g_{\omega B}\rho_B \\ &\quad - g_{\omega K}\rho_K \\ m_\rho^2\rho + 2\Lambda_v g_{\rho N}^2 g_{\omega N}^2\omega^2\rho &= \sum_B g_{\rho B}\tau_{3B}\rho_B - \frac{g_{\rho K}}{2}\rho_K, \end{aligned} \tag{7}$$

where ρ_N and ρ_N^S are the nucleon density and the scalar density, respectively and the kaon density $\rho_K = 2(\omega_K + g_{\omega K}\omega + \frac{g_{\rho K}}{2}\rho)K^*K$.

For the neutron matter with baryons and charged leptons, the β-equilibrium conditions are guaranteed with the following relations of chemical potentials for different particles:

$$\mu_p = \mu_{\Sigma^+} = \mu_n - \mu_e, \tag{8}$$

$$\mu_\Lambda = \mu_{\Sigma^0} = \mu_{\Xi^0} = \mu_n, \tag{9}$$

$$\mu_{\Sigma^-} = \mu_{\Xi^-} = \mu_n + \mu_e, \tag{10}$$

$$\mu_\mu = \mu_e, \tag{11}$$

and the charge neutrality condition is fulfilled by

$$n_p + n_\Sigma = n_e + n_{\mu^-} + n_{\Sigma^-} + n_{\Xi^-}. \tag{12}$$

The chemical potential of baryons and leptons reads

$$\mu_B = \sqrt{k_F^{B2} + m_B^{*2}} + g_{\omega B}\omega + g_{\rho B}\tau_{3B}\rho, \tag{13}$$

$$\mu_l = \sqrt{k_F^{l2} + m_l^2}, \tag{14}$$

where k_F^B is the Fermi momentum and the m_B^* is the effective mass of baryon B, which can be related to the scalar meson field as $m_B^* = m_B - g_{\sigma B}\sigma$, and k_F^l is the Fermi momentum of the lepton $l(\mu, \mathrm{e})$.

The total energy density of the system with kaon condensation reads then $\varepsilon = \varepsilon_N + \varepsilon_K$, where ε_N is the energy density of normal nuclear matter and can be given as

$$\begin{aligned} \varepsilon_B = &\sum_B \frac{2}{(2\pi)^3}\int_0^{K_F^B}\sqrt{m_B^* + k^2}d^3k + \frac{1}{2}m_\omega^2\omega^2 \\ &+ \frac{\xi}{8}g_{\omega N}^4\omega^4 + \frac{1}{2}m_\sigma^2\sigma^2 + \frac{\kappa}{6}g_{\sigma N}^3\sigma^3 + \frac{\lambda}{24}g_{\sigma N}^4\sigma^4 \\ &+ \frac{1}{2}m_\rho^2\rho^2 + 3\Lambda_v g_{\rho N}^2 g_{\omega N}^2\omega^2\rho^2 \\ &+ \frac{1}{\pi^2}\sum_l\int_0^{k_F^l}\sqrt{k^2 + m_l^2}k^2dk, \end{aligned} \tag{15}$$

where k_F^B is the Fermi momentum and m_B^* is the effective mass of baryons, which can be related to the scalar meson field as $m_B^* = m_B - g_{\sigma B}\sigma$. And the energy contributed by the kaon condensation ε_K is

$$\varepsilon_K = 2m_K^{*2}K^*K = m_K^*\rho_K. \tag{16}$$

The kaon does not contribute directly to the pressure as it is a (*s*-wave) Bose condensate so that the expression of pressure reads

$$\begin{aligned} P = &\sum_B \frac{1}{3}\frac{2}{(2\pi)^3}\int_0^{K_F^B}\frac{k^2}{\sqrt{m_B^{\star 2} + k^2}}dk^3 + \frac{1}{2}m_\omega^2\omega^2 \\ &+ \frac{\xi}{24}g_{\omega N}^4\omega^4 - \frac{1}{2}m_\sigma^2\sigma^2 - \frac{\kappa}{6}g_{\sigma N}^3\sigma^3 - \frac{\lambda}{24}g_{\sigma N}^4\sigma 4 \\ &+ \frac{1}{2}m_\rho^2\rho^2 + \Lambda_v g_{\rho N}^2 g_{\omega N}^2\omega^2\rho^2 \\ &+ \frac{1}{3\pi^2}\sum_l\int_0^{k_F^l}\frac{k^4}{\sqrt{k^2 + m_l^2}}dk. \end{aligned} \tag{17}$$

With the obtained ε and P, the mass-radius relation and other relevant quantities of the neutron star can be obtained by solving the Oppenheimer and Volkoff equation [10,49,50].

$$\begin{aligned} \frac{dP(r)}{dr} = &-\frac{GM(r)\varepsilon}{r^2}\left(1 + \frac{P}{\varepsilon C^2}\right)\left(1 + \frac{4\pi r^3 P}{M(r)C^2}\right) \\ &\times\left(1 - \frac{2GM(r)}{rC^2}\right)^{-1}, \end{aligned} \tag{18}$$

$$dM(r) = 4\pi r^2\varepsilon(r)dr, \tag{19}$$

where G is the gravitational constant and C is the velocity of light, and the EOS for neutron matter is given by Eq. (15) and

TABLE II. Parameter sets for the FSUGold model discussed in the text and the meson masses $M_\sigma = 491.5$ MeV, $M_\omega = 782.5$ MeV, $M_\rho = 763$ MeV.

Model	g_σ^2	g_ω^2	g_ρ^2	κ	λ	ξ	Λ_v
FSUGold	112.19	204.54	138.47	1.42	0.0238	0.06	0.03/0

Eq. (17); we can study the physical behavior of neutron stars for the extended model.

The σ-cut scheme [34], which is able to stiffen the EOS above saturation density, adds in the original Lagrangian density, the function [34,51,52]

$$\Delta U(\sigma) = \alpha \ln(1 + exp[\beta(f - f_{s,\text{core}})]), \tag{20}$$

where $f = g_{\sigma N}/M_N$ and $f_{s,\text{core}} = f_0 + c_\sigma(1 - f_0)$. M_N is the nucleon mass. f_0 is the value of f at saturation density, equal to 0.31 for the FSUGold model. c_σ is a positive parameter that we can adjust. The smaller c_σ is, the stronger the effect of the σ-cut scheme becomes. However, we must be careful that this scheme will not affect the saturation properties of nuclear matter. In this paper, we want to find a suitable value for the parameter c_σ that is able to satisfy the maximum mass constraint. α and β are constants, taken to be $4.822 \times 10^{-4} M_N^4$ and 120 as in Ref. [34]. This scheme stiffens the EOS by quenching the decreasing of the effective mass of the nucleon $M_N^* = M_N(1 - f)$ at high density.

Before giving our numerical results, we list parameters for the FSUGold model in Table II. The parameter of the models can be found in Refs. [30,33,53] in detail.

III. RESULTS

First, we want to find the range for c_σ in which the saturation properties of nucleon matter are not affected by the σ-cut scheme, by examining the effective mass of nucleons under the σ-cut scheme. In Fig. 1, we plot the ratio of the effective mass to the rest mass as a function of the baryon density, where ρ_0 is the saturation density 0.148 fm^{-3}. We can see that, when $\rho \leqslant \rho_0$, the effect mass is almost the same as nucleons-only matter and unchanged by the σ-cut scheme; when $\rho > \rho_0$, the effect mass dropped to around $0.55 M_N$.

In Fig. 2, we plot the σ meson field strength as a function of the baryon density with and without the σ-cut scheme. We must make sure that the σ potential is not affected by the σ-cut scheme at saturation density. It is clear that when the baryon density is below the saturation density, the σ meson field strength is almost the same as nucleons-only matter and unchanged by the σ-cut scheme. So we can conclude that, for $\rho > \rho_0$, the σ meson field strength is quenched at high baryon density, and the σ-cut scheme will not affect the saturation properties. This is what we want by using the σ-cut scheme. The smaller c_σ is, the stronger the quenching becomes.

Figure 3 shows the kaon energy(ω_k) and electron chemical potential(u_e) as a function of baryon density with $U_K = -120, -140, -160$ MeV for the parameters $\Lambda_v = 0$ and $\Lambda_v = 0.03$. K^- condensation initiates once the value of ω_K reaches that of the electron chemical potential. For $\Lambda_v = 0.03$, there is no intersection when $U_K = -120$ MeV.

Figure 4 shows the relative population of particles versus baryon density with kaon optical potential $U_K = -120, -140, -160$ MeV and $\Lambda_v = 0.03$. When $U_K = -120$ MeV, there is no K^-. For $U_K = -140$ MeV, the mixed phase initiates with the onset of K^- at $\sim 3.5\rho_0$ and terminates at $\sim 8.7\rho_0$; for $U_K = -160$ MeV, with the appearance of K^- at $\sim 2.7\rho_0$ and ceasing of electron population around $\sim 8.9\rho_0$, the proton and K^- population becomes equal following the charge neutrality condition. Σ^- will decrease and also Ξ^- will be delayed.

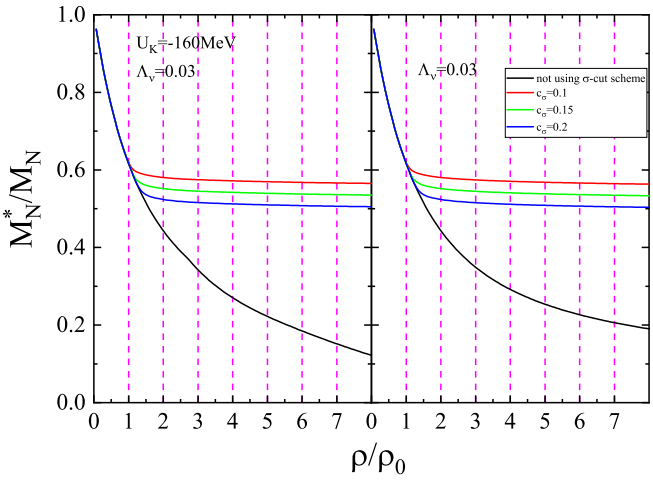

FIG. 1. Effective mass of nucleons versus baryon density in NS matter using and not using the σ-cut scheme. (Left panel) n, p, leptons, hyperons, K^-; (right panel) only n, p, leptons.

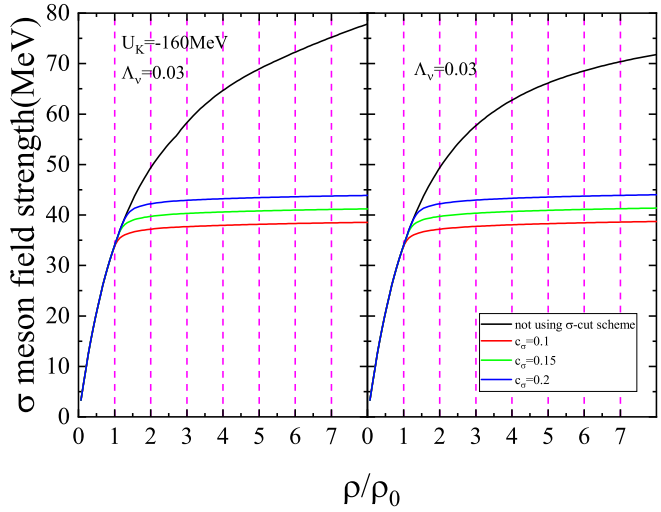

FIG. 2. σ meson field strength as a function of baryon density in NS matter using and not using the σ-cut scheme. (Left panel) n, p, leptons, hyperons, K^-; (right panel) only n, p, leptons.

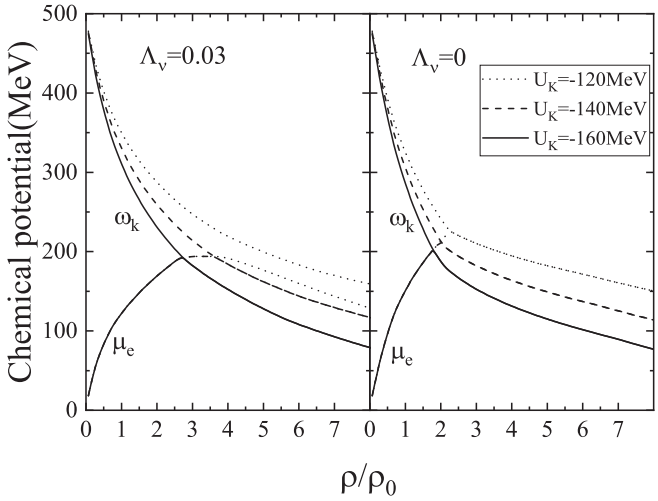

FIG. 3. Kaon energy(ω_k) and electron chemical potential(u_e) as a function of baryon density. (Left panel) $\Lambda_v = 0.03$; (right panel) $\Lambda_v = 0$. The solid curve shows $U_K = -160$ MeV, dotted lines show $U_K = -140$ MeV, and dashed lines show $U_K = -120$ MeV.

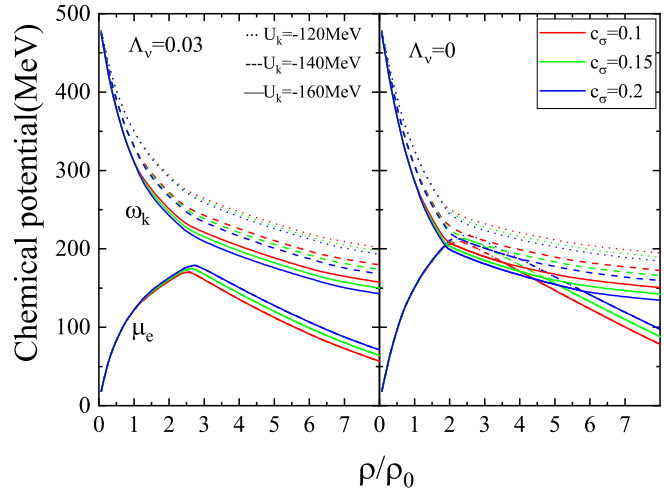

FIG. 5. Kaon energy(ω_k) and electron chemical potential(u_e) as functions of baryon density with the σ-cut scheme. (Left panel) Λ_v=0.03; (right panel) Λ_v=0. The solid curve shows $U_K = -160$ MeV, dotted lines show $U_K = -140$ MeV, and dashed lines show $U_K = -120$ MeV.

Next we examine the effect of the σ-cut scheme on the kaon energies. This is plotted in Fig. 5. For $\Lambda_v = 0.03$, there is no intersection between ω_K and μ_e. The bigger c_σ is, the closer ω_K and μ_e are. For $\Lambda_v = 0$, the kaon condensation will occur when $U_K = -140, -160$ MeV. The smaller c_σ is, the smaller σ meson field strength becomes; this will reduce the appearance of K^-. The isoscalar-isovector coupling (Λ_v) term in Eq. (1) is used to modify the density dependence of the symmetry energy and the neutron skin thicknesses of heavy nuclei; we can clearly find that Λ_v has a significant impact on the appearance of K^-. When $\Lambda_v = 0$, this will increase the chemical potential of the electron and promote the appearance of K^-.

It is interesting to know how the σ-cut scheme affects the relative populations of particles. In Fig. 6, the relative populations as a function of the baryon density are plotted

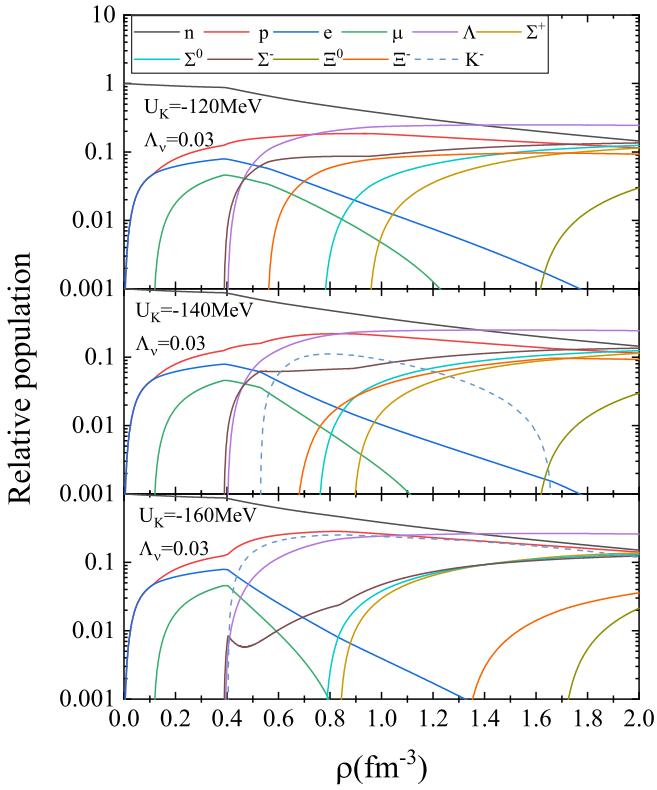

FIG. 4. Relative population of particles versus baryon density without the σ-cut scheme and K^- potential depth of $U_K = -120, -140, -160$ MeV. $\Lambda_v = 0.03$; dashed lines denote K^-.

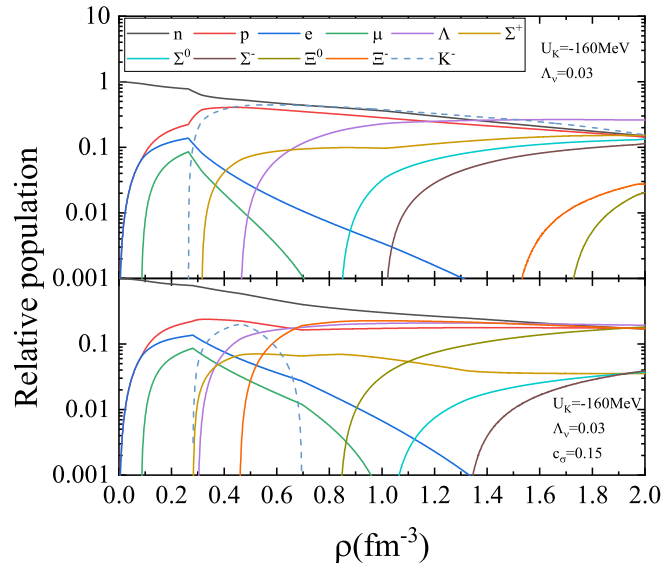

FIG. 6. Relative population of particles versus baryon density with and without the σ-cut scheme. K^- optical potential depth of $U_K = -160$ MeV, $\Lambda_v = 0$. (Upper panel) without the σ-cut scheme; (lower panel) $c_\sigma = 0.15$; dashed lines denote K^-.

TABLE III. Threshold densities n_{cr} (in units of fm^{-3}) for kaon condensation in dense nuclear matter for different values of K^- optical potential depths U_K (in units of MeV) without the σ-cut scheme and $c_\sigma = 0.15$.

U_K	$n_{cr}(K^-)$ (no σ-cut scheme)		$n_{cr}(K^-)(c_\sigma = 0.15)$	
(MeV)	$\Lambda_v = 0.03$	$\Lambda_v = 0$	$\Lambda_v = 0.03$	$\Lambda_v = 0$
-120	None	0.34	None	None
-140	0.54	0.3	None	0.36
-160	0.41	0.27	None	0.28

with K^- optical potential $U_K = -160$ MeV, we are interested in the occurrence of K^-, so we choose $\Lambda_v = 0$. We can find that the percentage of K^- is decreased by the σ-cut scheme, and the relative populations of some hyperons are influenced significantly by the σ-cut scheme when $\Lambda_v = 0$. The σ-cut scheme increases the percentages of Ξ^- and Ξ^0, while it decreases the percentages of Σ^- and Σ^0. We list the threshold densities n_{cr} for kaon condensation for different values of K^- optical potential depths U_K in Table III.

Then we can discuss some properties of the neutron star. Figure 7 shows the matter pressure as a function of energy density for the kaon optical potential $U_K = -120, -140, -160$ MeV and without the σ-cut scheme. The appearance of kaon to a great extent softens the EOS. As the energy density increases, the EOS of NS matter that contains K mesons will exceed that of only nucleons and hyperons.

The parameter Λ_v describing the interaction between ρ meson and ω meson in the FSUGold model is introduced to soften the symmetry energy. It can affect the macroscopic properties of the neutron stars. In Fig. 8 the EOS is displayed for $\Lambda_v = 0$ and $\Lambda_v = 0.03$. We can find that the EOS with parameter $\Lambda_v = 0$ is softer than the case of $\Lambda_v = 0.03$, by

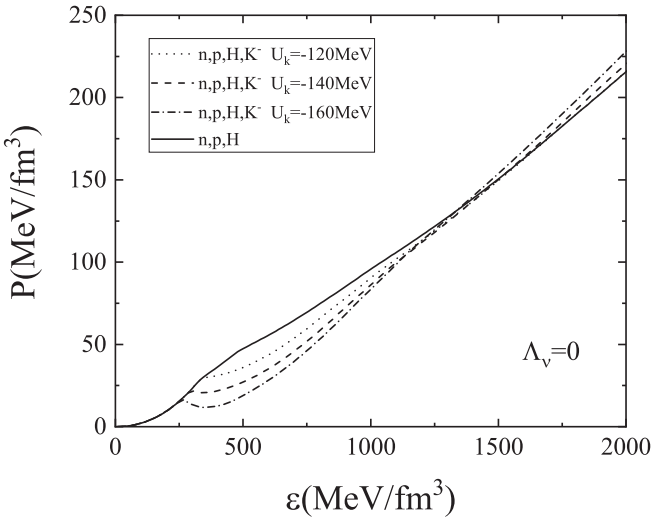

FIG. 7. Pressure versus energy density without the σ-cut scheme. The solid line is for n, p, leptons, and hyperons whereas others are with additional K^-. Dotted line shows $U_K = -120$ MeV, dashed line shows $U_K = -140$ MeV, and dash-dotted line shows $U_K = -160$ MeV.

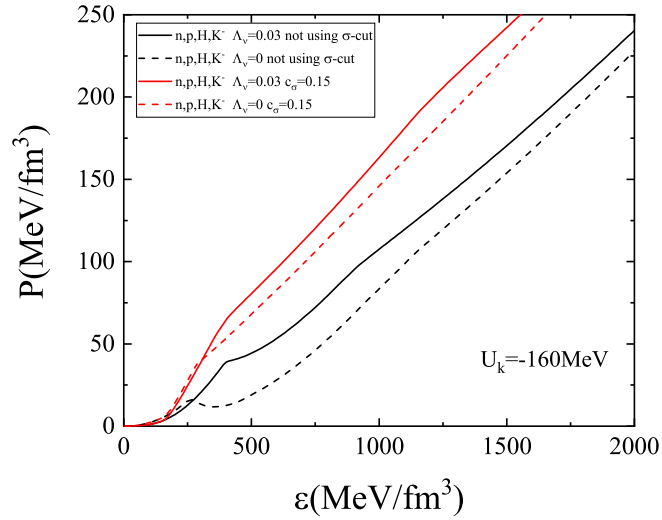

FIG. 8. Pressure versus energy density with and without the σ-cut scheme. The solid lines curve with $\Lambda_v = 0.03$, dashed lines curve with $\Lambda_v = 0$, the black lines are without the σ-cut scheme, and the red lines are with $c_\sigma = 0.15$.

using the σ-cut scheme; the EOS is significantly stiffened when $c_\sigma = 0.15$. The results of the mass-radius relation for static spherical stars from the solution of the Tolman-Oppenheimer-Volkoff (TOV) equation discussed here are shown in Fig. 9. The mass measurements of PSR J1614−2230 [1–4], PSR J0348+0432 [5], MSP J0740+6620, and PSR J0030−0451 are indicated by the horizontal bars. We find that this scheme can significantly increase the maximum mass of the neutron star. The smaller c_σ is, the stronger the effect of this scheme is. The parameter Λ_v will not significantly affect

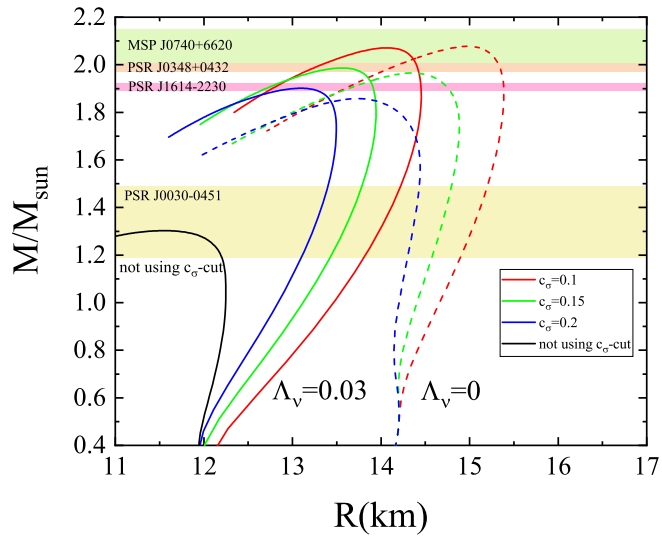

FIG. 9. Mass-radius relation using and not using the σ-cut scheme in NS matter including hyperons and K^-. The solid lines denote $\Lambda_v = 0.03$, dashed lines denote $\Lambda_v = 0$, and $U_K = -160$ MeV. The horizontal bars indicate the observational constraints of PSR J1614−2230 [1,4], PSR J0348+0432 [5], MSP J0740+6620 [6,7], and PSR J0030−0451 [54].

TABLE IV. The maximum mass (in units of solar mass $M_\odot$) and radius (in units of km) of neutron stars using and not using the σ-cut scheme.

	$\Lambda_v = 0.03$		$\Lambda_v = 0$		MSP J0740+6620		PSR J0030−0451	
	M	R	M	R	M	R	M	R
No c_σ-cut scheme(n, p, H)	1.31	11.6	1.32	13.3	2.08 ± 0.07	$12.39^{+1.3}_{-0.98}$	$1.34^{+0.15}_{-0.16}$	$12.71^{+1.14}_{-1.19}$
$c_\sigma = 0.1(n, p, H, K^-)$	2.07	14.1	2.07	15.1				
$c_\sigma = 0.15(n, p, H, K^-)$	1.99	13.6	1.96	14.4				
$c_\sigma = 0.2(n, p, H, K^-)$	1.9	13.1	1.86	13.7				

the maximum mass of the neutron star, but will increases the radius; note that there is no appearance of K^- when $\Lambda_v = 0.03$ from Fig. 5. We list the simultaneous measurement of radius for MSP J0740 + 6620 [6,7] and PSR J0030−0451 [54] by the NICER data and maximum mass of the neutron star for various values of c_σ and Λ_v in Table IV.

IV. SUMMARY

In this paper, we have discussed the K^- meson condensation inside the neutron star under the FSUGold model. This model predicts a limiting neutron star mass of $1.72M_\odot$ [29]. The maximum mass changes to $1.3M_\odot$ when hyperons are included [13]. Adding kaon meson will further soften the EOS. In this work we used the σ-cut scheme; by adjusting the parameter c_σ, we got the maximum mass heavier than $2M_\odot$ within the range of observed mass measurements. We also compared the radius of NS with the recent NICER results; the ρ-ω coupling constant Λ_v has a significant effect on the radius with the appearance of K^- and when using the σ-cut scheme. The kaon condensation cannot exist in the NS matter for $\Lambda_v = 0.03$; for $\Lambda_v = 0$, as the $\rho - \omega$ interaction is switched off, the electron chemical potential will increase and make it possible for K^- condensation to occur in the neutron star.

[1] P. Demorest, T. Pennucci, S. Ransom, M. Roberts, and J. Hessels, Shapiro delay measurement of a two solar mass neutron star, Nature (London) **467**, 1081 (2010).

[2] Z. Arzoumanian, A. Brazier, S. Burke-Spolaor, S. Chamberlin, S. Chatterjee, B. Christy, J. M. Cordes, N. J. Cornish, F. Crawford, H. T. Cromartie *et al.*, The nanograv 11-year data set: High-precision timing of 45 millisecond pulsars, Astrophys. J. Suppl. Ser. **235**, 37 (2018).

[3] E. Fonseca, T. T. Pennucci, J. A. Ellis, I. H. Stairs, D. J. Nice, S. M. Ransom, P. B. Demorest, Z. Arzoumanian, K. Crowter, T. Dolch *et al.*, The nanograv nine-year data set: Mass and geometric measurements of binary millisecond pulsars, Astrophys. J. **832**, 167 (2016).

[4] F. Özel, D. Psaltis, S. Ransom, P. Demorest, and M. Alford, The massive pulsar PSR J1614–2230: Linking quantum chromodynamics, gamma-ray bursts, and gravitational wave astronomy, Astrophys. J. Lett. **724**, L199 (2010).

[5] J. Antoniadis, P. C. C. Freire, N. Wex, T. M. Tauris, R. S. Lynch, M. H. van Kerkwijk, M. Kramer, C. Bassa, V. S. Dhillon, T. Driebe *et al.*, A massive pulsar in a compact relativistic binary, Science **340**, 1233232 (2013).

[6] E. Fonseca, H. Cromartie, T. T. Pennucci, P. S. Ray, A. Y. Kirichenko, S. M. Ransom, P. B. Demorest, I. H. Stairs, Z. Arzoumanian, L. Guillemot *et al.*, Refined mass and geometric measurements of the high-mass PSR J0740+ 6620, Astrophys. J. Lett. **915**, L12 (2021).

[7] H. T. Cromartie, E. Fonseca, S. M. Ransom, P. B. Demorest, Z. Arzoumanian, H. Blumer, P. R. Brook, M. E. DeCesar, T. Dolch, J. A. Ellis *et al.*, Relativistic Shapiro delay measurements of an extremely massive millisecond pulsar, Nat. Astronomy **4**, 72 (2020).

[8] T. E. Riley, A. L. Watts, P. S. Ray, S. Bogdanov, S. Guillot, S. M. Morsink, A. V. Bilous, Z. Arzoumanian, D. Choudhury, J. S. Deneva *et al.*, A nicer view of the massive pulsar PSR J0740+ 6620 informed by radio timing and xmm-newton spectroscopy, Astrophys. J. Lett. **918**, L27 (2021).

[9] R. Abbott, T. D. Abbott, S. Abraham, F. Acernese, K. Ackley, C. Adams, R. X. Adhikari, V. B. Adya, C. Affeldt, M. Agathos *et al.*, GW190814: Gravitational waves from the coalescence of a 23 solar mass black hole with a 2.6 solar mass compact object, Astrophys. J. Lett. **896**, L44 (2020).

[10] N. K. Glendenning, *Compact Stars: Nuclear Physics, Particle Physics and General Relativity* (Springer Science & Business Media, Berlin, Heidelberg, 2012).

[11] F. Weber, R. Negreiros, P. Rosenfield, and M. Stejner, Pulsars as astrophysical laboratories for nuclear and particle physics, Prog. Part. Nucl. Phys. **59**, 94 (2007).

[12] J. Schaffner and I. N. Mishustin, Hyperon rich matter in neutron stars, Phys. Rev. C **53**, 1416 (1996).

[13] C. Wu and Z. Ren, Strange hadronic stars in relativistic mean-field theory with the FSUGold parameter set, Phys. Rev. C **83**, 025805 (2011).

[14] S. Pal, M. Hanauske, I. Zakout, H. Stoecker, and W. Greiner, Neutron star properties in the quark meson coupling model, Phys. Rev. C **60**, 015802 (1999).

[15] N. K. Glendenning and F. Weber, Nuclear solid crust on rotating strange quark stars, Astrophys. J. **400**, 647 (1992).

[16] N. K. Glendenning, A Crystalline quark - hadron mixed phase in neutron stars, Phys. Rept. **264**, 143 (1996).

[17] H. Li, X.-L. Luo, Y. Jiang, and H.-S. Zong, Model study of a quark star, Phys. Rev. D **83**, 025012 (2011).

[18] H. Li, X.-L. Luo, and H.-S. Zong, Bag model and quark star, Phys. Rev. D **82**, 065017 (2010).

[19] V. B. Thapa and M. Sinha, Dense matter equation of state of a massive neutron star with anti-kaon condensation, Phys. Rev. D **102**, 123007 (2020).

[20] T. Maruyama, T. Tatsumi, D. N. Voskresensky, T. Tanigawa, T. Endo, and S. Chiba, Finite size effects on kaonic pasta structures, Phys. Rev. C **73**, 035802 (2006).
[21] G. E. Brown, C.-H. Lee, H.-J. Park, and M. Rho, Study of Strangeness Condensation by Expanding About the Fixed Point of the Harada-Yamawaki Vector Manifestation, Phys. Rev. Lett. **96**, 062303 (2006).
[22] G.-y. Shao and Y.-x. Liu, Influence of the isovector-scalar channel interaction on neutron star matter with hyperons and antikaon condensation, Phys. Rev. C **82**, 055801 (2010).
[23] D. B. Kaplan and A. E. Nelson, Strange goings on in dense nucleonic matter, Phys. Lett. B **175**, 57 (1986).
[24] A. E. Nelson and D. B. Kaplan, Strange condensate realignment in relativistic heavy ion collisions, Phys. Lett. B **192**, 193 (1987).
[25] N. K. Glendenning, Neutron stars are giant hypernuclei? Astrophys. J. **293**, 470 (1985).
[26] J. D. Walecka, A Theory of highly condensed matter, Ann. Phys. **83**, 491 (1974).
[27] D. Vautherin and D. M. Brink, Hartree-Fock calculations with Skyrme's interaction. 1. Spherical nuclei, Phys. Rev. C **5**, 626 (1972).
[28] H. Shen, H. Toki, K. Oyamatsu, and K. Sumiyoshi, Relativistic equation of state of nuclear matter for supernova and neutron star, Nucl. Phys. A **637**, 435 (1998).
[29] B. G. Todd-Rutel and J. Piekarewicz, Neutron-Rich Nuclei and Neutron Stars: A New Accurately Calibrated Interaction for the Study of Neutron-Rich Matter, Phys. Rev. Lett. **95**, 122501 (2005).
[30] F. J. Fattoyev, C. J. Horowitz, J. Piekarewicz, and G. Shen, Relativistic effective interaction for nuclei, giant resonances, and neutron stars, Phys. Rev. C **82**, 055803 (2010).
[31] J. Piekarewicz, Why is Tin so soft? Phys. Rev. C **76**, 031301(R) (2007).
[32] J. Piekarewicz, Validating relativistic models of nuclear structure against theoretical, experimental, and observational constraints, Phys. Rev. C **76**, 064310 (2007).
[33] F. J. Fattoyev and J. Piekarewicz, Relativistic models of the neutron-star matter equation of state, Phys. Rev. C **82**, 025805 (2010).
[34] K. A. Maslov, E. E. Kolomeitsev, and D. N. Voskresensky, Making a soft relativistic mean-field equation of state stiffer at high density, Phys. Rev. C **92**, 052801(R) (2015).
[35] P. Char and S. Banik, Massive neutron stars with antikaon condensates in a density dependent hadron field theory, Phys. Rev. C **90**, 015801 (2014).
[36] N. K. Glendenning and J. Schaffner-Bielich, First order kaon condensate, Phys. Rev. C **60**, 025803 (1999).
[37] N. K. Glendenning and J. Schaffner-Bielich, Kaon Condensation and Dynamical Nucleons in Neutron Stars, Phys. Rev. Lett. **81**, 4564 (1998).
[38] G.-Q. Li, C. H. Lee, and G. E. Brown, Kaons in dense matter, kaon production in heavy ion collisions, and kaon condensation in neutron stars, Nucl. Phys. A **625**, 372 (1997).
[39] S. Pal, C. M. Ko, Zi-wei Lin, and B. Zhang, Antiflow of kaons in relativistic heavy ion collisions, Phys. Rev. C **62**, 061903(R) (2000).
[40] T. Waas and W. Weise, S wave interactions of anti-K and eta mesons in nuclear matter, Nucl. Phys. A **625**, 287 (1997).
[41] V. Koch, K^--proton scattering and the Λ (1405) in dense matter, Phys. Lett. B **337**, 7 (1994).
[42] M. Lutz, Nuclear kaon dynamics, Phys. Lett. B **426**, 12 (1998).
[43] A. Ramos and E. Oset, The Properties of anti-K in the nuclear medium, Nucl. Phys. A **671**, 481 (2000).
[44] L. Tolos, A. Ramos, and A. Polls, The Anti-kaon nuclear potential in hot and dense matter, Phys. Rev. C **65**, 054907 (2002).
[45] E. Friedman, A. Gal, and J. Mares, K- Nucleus relativistic mean field potential consistent with kaonic atoms, Phys. Rev. C **60**, 024314 (1999).
[46] J. Schaffner, C. B. Dover, A. Gal, C. Greiner, D. J. Millener, and H. Stoecker, Multiply strange nuclear systems, Ann. Phys. **235**, 35 (1994).
[47] D. J. Millener, C. B. Dover, and A. Gal, Lambda nucleus single particle potentials, Phys. Rev. C **38**, 2700 (1988).
[48] T. Malik, S. Banik, and D. Bandyopadhyay, Equation-of-state table with hyperon and antikaon for supernova and neutron star merger, Astrophys. J. **910**, 96 (2021).
[49] M. Baldo, I. Bombaci, and G. F. Burgio, Microscopic nuclear equation of state with three-body forces and neutron star structure, Astron. Astrophys. **328**, 274 (1997).
[50] J. R. Oppenheimer and G. M. Volkoff, On massive neutron cores, Phys. Rev. **55**, 374 (1939).
[51] M. Dutra, O. Lourenço, and D. P. Menezes, Stellar properties and nuclear matter constraints, Phys. Rev. C **93**, 025806 (2016); **94**, 049901(E) (2016).
[52] E. E. Kolomeitsev, K. A. Maslov, and D. N. Voskresensky, Hyperon puzzle and the RMF model with scaled hadron masses and coupling constants, J. Phys.: Conf. Ser. **668**, 012064 (2016).
[53] F. J. Fattoyev and J. Piekarewicz, Sensitivity of the moment of inertia of neutron stars to the equation of state of neutron-rich matter, Phys. Rev. C **82**, 025810 (2010).
[54] T. E. Riley, A. L. Watts, S. Bogdanov, P. S. Ray, R. M. Ludlam, S. Guillot, Z. Arzoumanian, C. L. Baker, A. V. Bilous, D. Chakrabarty, K. C. Gendreau, A. K. Harding, W. C. G. Ho, J. M. Lattimer, S. M. Morsink, and T. E. Strohmayer, A nicer view of PSR J0030−0451: Millisecond pulsar parameter estimation, Astrophys. J. **887**, L21 (2019).